EFFECT OF RU ADDITION ON CAST NICKEL BASE SUPERALLOY WITH LOW CONTENT OF CR AND HIGH CONTENT OF W

Yunrong Zheng, Xiaoping Wang, Jianxin Dong, and Yafang Han,
Institute of Aeronautical Materials, Beijing 100095, CHINA

H. Murakami and H. Harada
National Research Institute for Metals, 1-2-1, Sengen, Tsukuba, JAPAN

Abstract

The effect of Ru on two kinds of cast nickel-base superalloys in as-cast, heat-treated and oxidation tested specimens has been characterised by optical metallography and scanning electron microscopy. The evaluation of microstructure confirms the distribution of Ru in various phases, the beneficial role of Ru in stabilising microstructure, delaying formation of M_6C and increasing incipient melting temperature of the alloys. The role of Ru on oxidation resistance is different in various kinds of alloy; in Hf-bearing alloys, it has a beneficial effect, but in a 1.5% Cr alloy, the effect of Ru is not obvious.

Introduction

An important aim of developing new cast Ni-base superalloys is to increase the operating temperature of these alloys. One of the most effective ways to increase the stress rupture strength at temperatures above 1050°C is to decrease the content of Cr and increase the content of W in cast Ni-base superalloys. For example, in the third generation of single crystal superalloys, the content of Cr has been decreased to the level of 2-4wt%, and the total amount of refractory elements of W, Mo, Ta and Re is as high as 20wt% [1]. Among these refractory elements, Re is a unique element which can increase both the high temperature stress rupture strength and the oxidation resistance of the alloys. Re was first used in a conventional casting superalloy NASAII [2], and subsequently used in SC superalloys with Re content of 3-6wt%[1]. In BIAM, in order to develop a low cost Re-free casting Ni base superalloy 601, which has the stress rupture life of 50h under 1100 °C/118MPa, the content of W was increased to 16wt%, and the content of Cr was decreased to 1.5wt%[3]. However, the decrease of Cr content led to a decrease of oxidation resistance of this alloy, which should be compensated by addition of other oxidation resistant elements.

It has been found that Ru was a potential alloying element to increase the oxidation resistance, and can replace part of the Re due to its relatively lower density and cost compared with Re [4]. Since Ru belongs to the Pt family, it has high chemical stability and hence high oxidation resistance. Furthermore, Ru can strengthen both γ' and γ phases effectively due to its large atomic radius. Based on the above-mentioned considerations, this study was performed.

Experimental procedure

Two kinds of alloys were selected in order to study the role of Ru; their chemical compositions were listed in Table 1. Alloy 1 is a commercially cast superalloy K19H containing Hf, alloy 3 is a trial cast superalloy with low Cr, high W content selected on the basis of the stress rupture properties under the condition of 1100°C/118Mpa. Alloy 2 and alloy 4 are both Ru-bearing modified alloys from alloy 1 and alloy 3 respectively.

Table 1 Chemical compositions of tested alloys, wt.%

Alloy	Co	Cr	Mo	W	Nb	Ru	Al	Ti	Hf	C	B	Ni
1	11.8	6.0	1.9	10.3	2.3	-	5.8	1.4	1.3	0.12	0.02	bal.
2	11.8	6.0	1.9	10.3	2.3	3.0	5.8	1.4	1.3	0.12	0.02	bal.
3	9.6	1.3	1.3	16.2	1.0	-	6.0	1.1	-	0.10	0.024	bal.
4	9.6	1.3	1.3	16.2	1.0	3.0	6.0	1.1	-	0.10	0.024	bal.

The distribution of Ru, dendrite segregation and phase precipitation were analysed using optical microscopy (OM) and SEM/EDX for all the alloys. The effect of Ru on the oxidation resistance was investigated by static oxidation test at the temperature of 1100°C, the composition and morphology of the surface oxide scale after oxidation testing were analysed by using the LV method of SEM. The microstructures after long-time exposure at 1100 °C for 100 hours were observed for all alloys. In order to determine the influence of Ru on the solid solutioning of γ' and the incipient melting point of alloys, the directionally solidified alloys 3 and 4 were heat-treated in the temperature range of 1260-1300°C, and thus a suitable solid solutioning treatment was determined.

Results and discussion

Composition selection of trial alloys

The chemical composition of alloy 3 in Table 1 was designed on the basis of the compositions of K19H alloy (6Cr-10W), by decreasing Cr content to 1.5wt% and increasing the total content of W+Mo+Nb+Ta up to 20wt%. The chemical compositions of these designed conventional cast alloys and their stress rupture lives are given in Table 2. It is shown from Table 2 that the strength level of alloy A is lower than that of alloys B and C. The precipitation of primary μ and α (W, Mo) phases

was observed in alloy D due to excessive alloying. The alloy C contains higher Ta which causes an increment of primary eutectic (γ+γ') phases (Fig.1) and leads to difficulty of solid solutioning treatment. Moreover, Ta is a high cost element; therefore, alloy B is selected as a trial alloy and named as alloy 3 in Table 1.

Distribution of Ru

The distributions of Ru in the precipitated phases, dendrite and interdendrite regions in alloys 2 and 4 are shown in Table 3.

The compositions of γ' and γ in alloy 4 were determined when γ' and γ were coarser after 1100°C /100h long-term exposure, and the compositions of M_6C carbides were determined from specimens after higher temperature treatment of 1300°C.

It can be seen from Table 3 that Ru hardly enters MC carbides, and the solubility of Ru in the M_6C carbides is higher than that in the MC carbides. However, Ru has a rather higher solubility in the γ' and Ni_5Hf phases. The Ru concentration in the eutectic γ' phase is higher than in the secondary γ' phase, and higher in the γ matrix compared with the secondary γ' phase. The partitioning ratio of (γ/γ') is near 1:0.7. Ru is uniformly distributed between dendritic and interdendrtic regions.

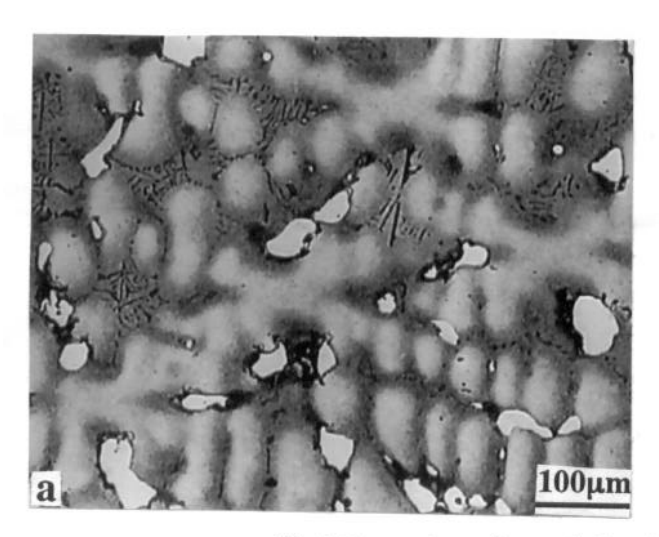Table 2 Chemical compositions of trial alloys and stress rupture lives

Alloy	Cr	Co	W	Mo	Al	Ti	Nb	Ta	C	B	Ni	Stress rupture life (h) 118MPa	
												1080°C	1100°C
A	3.0	9.9	14.0	1.9	5.6	1.2	2.5	-	0.14	0.02	bal	61.4, 80.1	
B	1.3	9.6	16.2	2.1	6.0	1.1	1.0	-	0.10	0.024	bal		51.3, 52.4
C	1.5	9.8	16.2	2.0	4.9	1.1	1.1	4.4	0.10	0.034	bal		65.0, 52.1
D	1.4	9.6	16.0	2.0	5.0	1.1	1.0	6.7	0.10	0.02	bal		40.0, 41.4

Table 3 Distribution of Ru in as-cast alloys 2 and 4, wt%

Alloy	Eutectic γ'	γ'	γ	Ni_5Hf	MC	M_6C	dendrite	interdendrite
2	2.94	-	-	2.13	0.23	-	2.96	3.06
4	2.51	2.14*	2.97*	-	0.15	0.87**	2.68	2.78

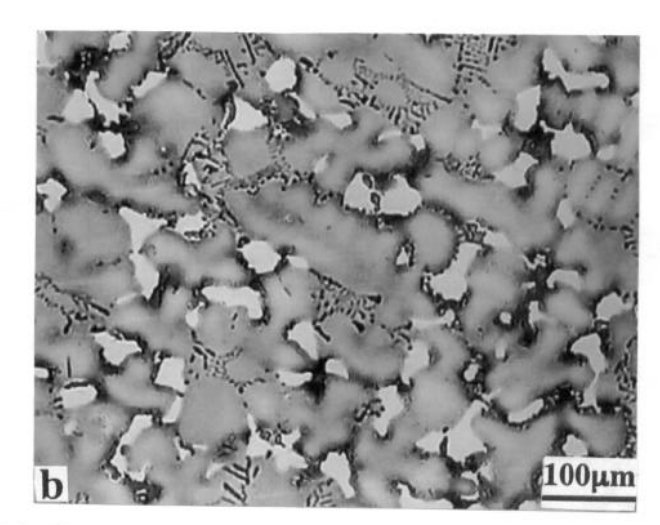* After 1100°C/100h heat exposure
** After 1300°C/4h heat treatment

306

Fig.1 Comparison of eutectic ($\gamma + \gamma'$) in alloys; (a) alloy B, (b) alloy C.

Effect of Ru on microstructure

Addition of 3wt.% Ru in alloys 2 and 4 seems to have no effect on the as-cast microstructures, while it delays the precipitation of M_6C carbides. After heat treatment at $1100^{\circ}C/50h$ for alloy 3, large amount of coarse-granular or a few short-plate M_6C carbide particles precipitated along grain boundaries and interdendritic regions (Fig.2). For alloy 4 exposed at $1100^{\circ}C/100h$, only at some grain boundary segments were M_6C particles detected (Fig.3a), and a strong raft tendency of the γ' phase was observed at the dendritic areas (Fig.3b).

Partial solid solution of γ' phases in dendrites takes place during heat treatment of $1260^{\circ}C/4h$ of alloys 3 and 4. The secondary γ' phase was completely dissolved except for eutectic γ' phases in alloy 4 at treatment of $1280^{\circ}C/4h$. For alloy 3, a few secondary γ' phases existing in the vicinity of the eutectic γ' were observed, and some neck-like M_6C carbides enveloped by γ' film existed (Fig.4).

With increasing temperature to $1300^{\circ}C$ for 4h, all kinds of γ' phases were dissolved, but the incipient melting phenomenon apparently occurred in two of the alloys. Compared to alloy 3, the degree of incipient melting of alloy 4 is lower and it takes place only in some eutectic γ'. For alloy 3, large parts of the original eutectic ($\gamma+\gamma'$) region and some columnar grain boundary were melted. The morphology of the incipient melting zone in both alloys is shown in Fig.5. It can be seen from Fig.5 that some block shape or coarse plate M_6C carbides often appeared in the incipient melting zone and its adjacent zone, especially in alloy 3. Element W is the main composition of M_6C carbide and a typical content of

metal element in M_6C carbide of alloy 4 is 72.3W-6.7Mo-11.2Ni-3.4Co-1.7Al-0.9Ru-0.7Cr-0.2Ti, This proves that Ru is not a M_6C carbide former.

Oxidation resistance of alloys

Fig.6 shows the experimental results of oxidation tests for the four alloys, Fig.6b is a magnification of Fig.6a. The role of Ru is different in various kinds of alloys. For Hf-bearing alloys, Ru decreases the rate of weight gain slightly, but can drop the rate of weight loss during oxidation testing at $1100^{\circ}C$. The value of the weight gain decreases from $6.87g/m^2$ to $1.55g/m^2$ in alloy 1 compared with alloy 2 after oxidation test at $1100^{\circ}C$ for 65h due to the decreased flaking of oxide scale.

Observation from SEM has shown that the oxide scale on the surface is porous and contains a crystallographic slope in the Ru-free alloy, as shown in Fig.7a, whereas, the scale of the Ru-bearing alloy is denser and there are nodules existing on some local regions (Fig.7b). On cross sections of the oxidation layer, the continuous scale was observed in alloy 2 (Fig.8a).

For low Cr alloys, the weight gain was increased during the first 3 hours; even alloy 4 has a larger weight gain. However, spalling of the scale in alloy 4 was later than that of alloy 3. Once spalling of the scale appeared five hours later, the weight loss rate was at the same level in alloys 3 and 4, about $8.1g/m^2\cdot h$. The continuous scale did not appeared in alloys 3 and 4, this is apparent from Fig.8b, which shows the serious inter-oxidation in the low Cr alloy. The compositions of the oxidation layer at alloy 4 after the oxidation test of $1100^{\circ}C/50h$ is listed in Table 4.
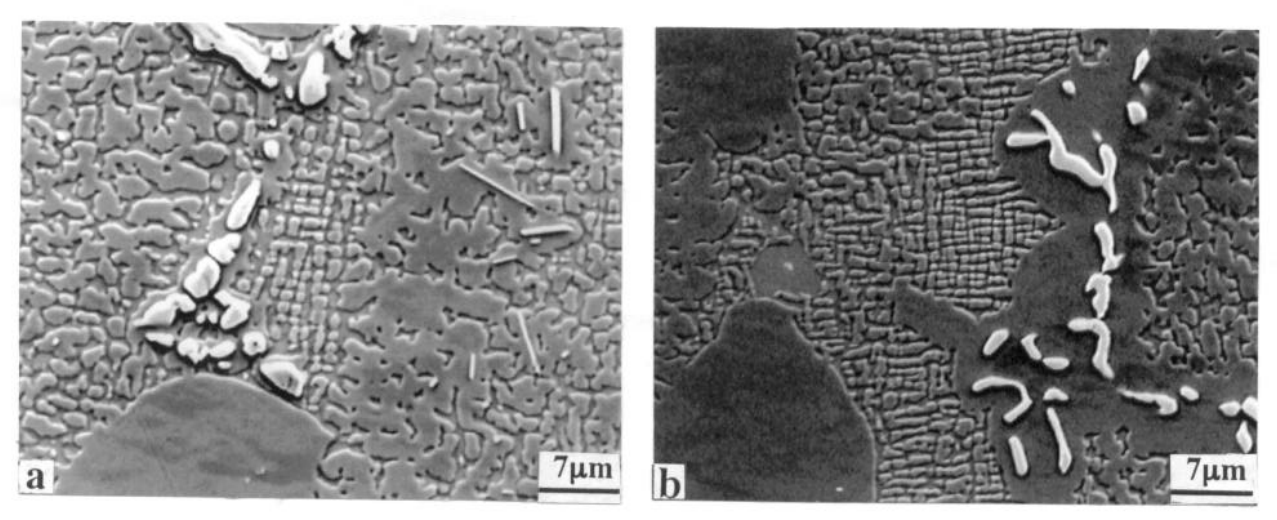
Fig.2 M$_6$C carbide precipitated from alloy 3 after 1100°C for 50h;
(a) granular and short-plate M$_6$C carbide at interdendrite, (b) M$_6$C along grain boundaries.
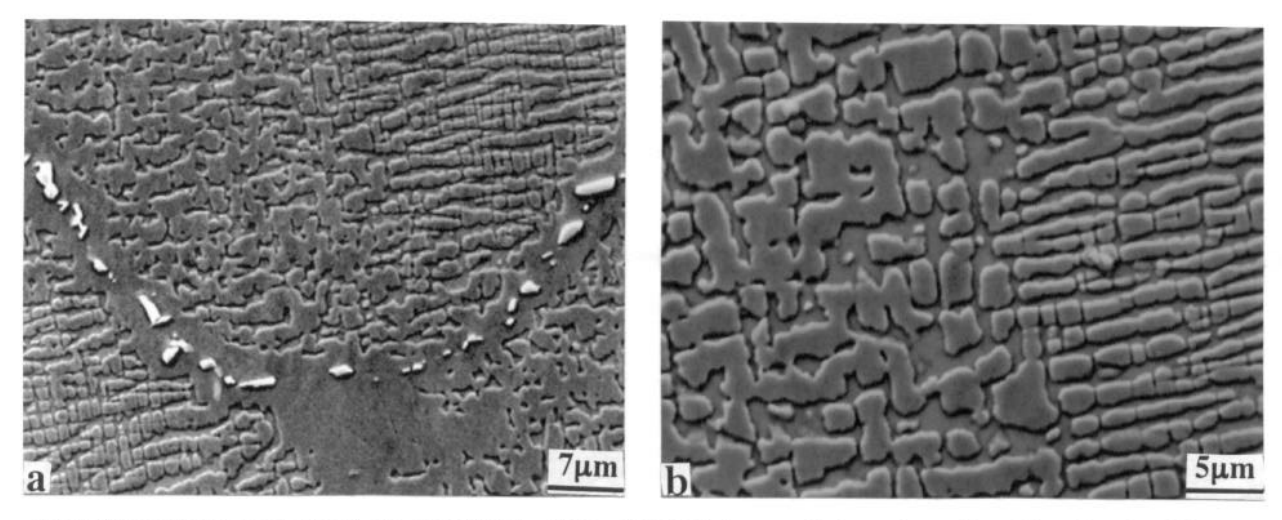

Fig.3 Microstructure of alloy 4 after 1100°C for 100h; (a) M$_6$C along grain boundary, (b) rafting γ' at dendrite.
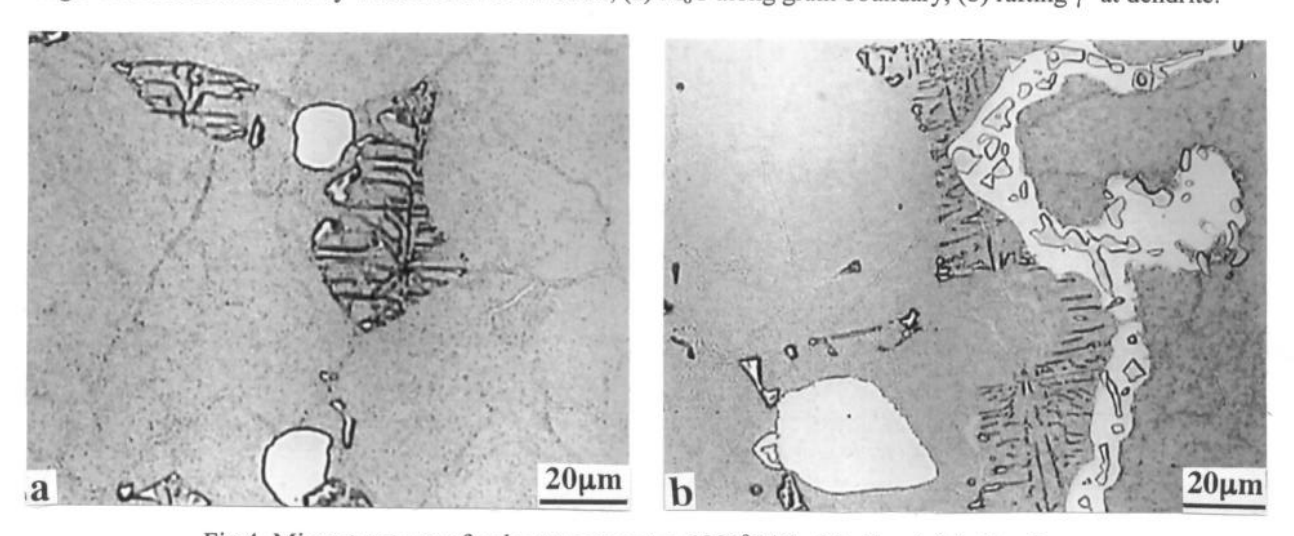

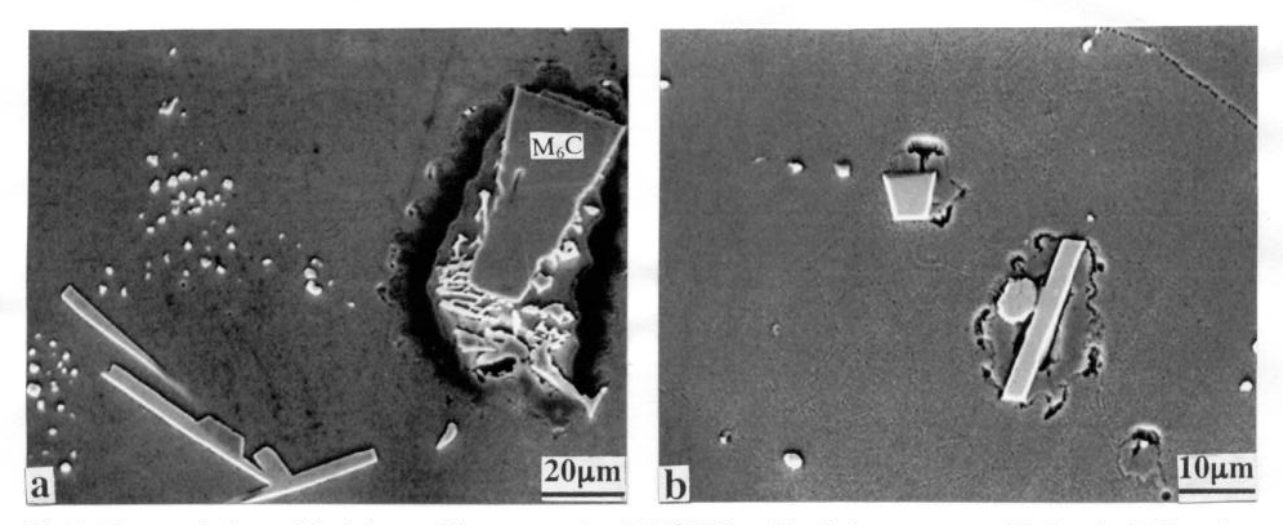Fig.4 Microstructures after heat treatment at 1280°C/4h; (a) alloy 4 (b) alloy 3.

Fig.5 The morphology of incipient melting zones after 1300°C/4h solid solution treatment; (a)alloy 3, (b)alloy 4
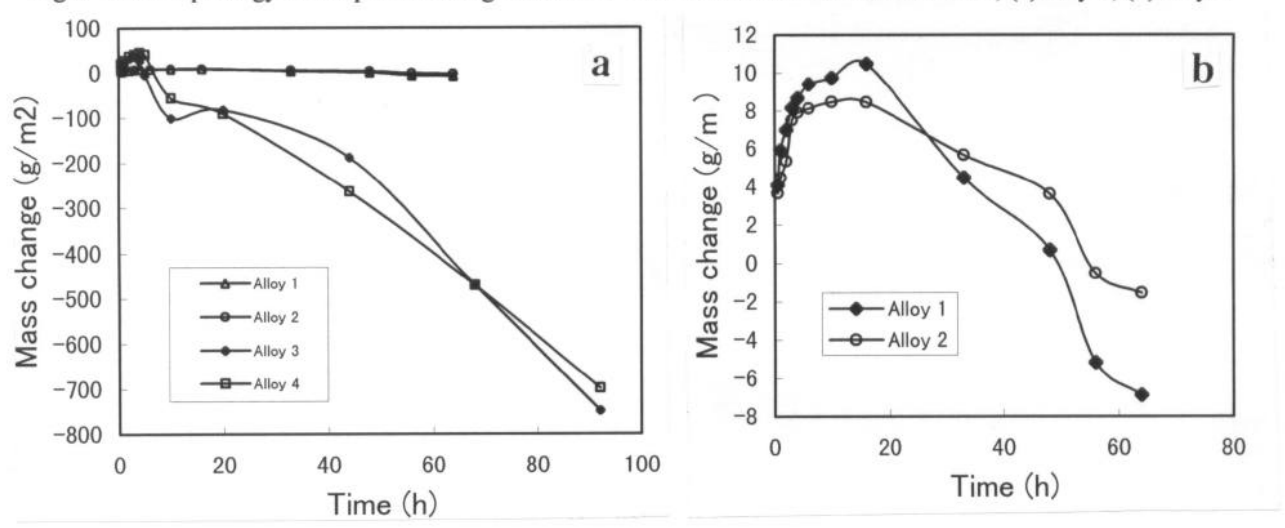

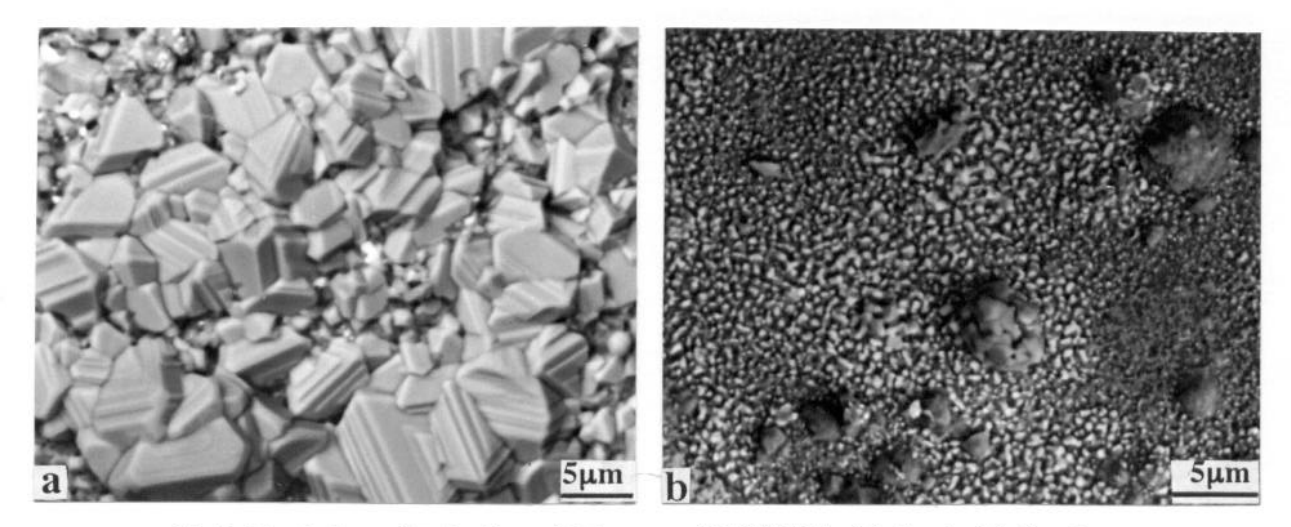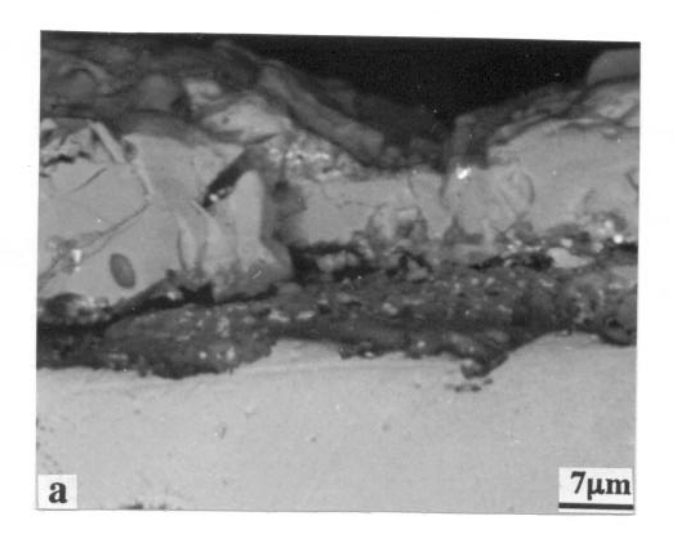Fig.6 Weight change of alloys during oxidation test at 1100 °C

Fig.7 Morphology of scale after oxidation test of 1100°C/65h; (a) alloy 1 (b) alloy 2.
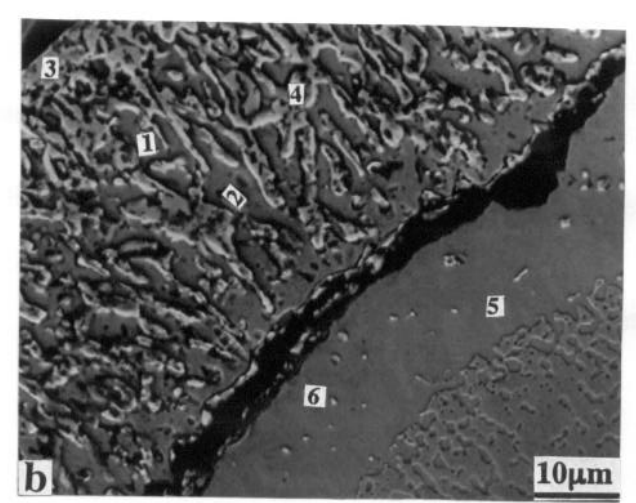
Fig.8 Morphology of oxide layer on alloys after oxidation test at 1100 °C/50h, (a) alloy 2 (b) alloy 4.

Table 4 Compositions of oxidation layer on alloy 4 after test of 1100°C/50h.

Point	O	Al	Nb	Mo	Ru	Ti	Cr	Co	Ni	W
1	2.26	0.21	0.36	1.35	4.26	0.22	0.35	2.69	84.67	3.63
2	2.22	0.17	0.22	0.83	3.57	0.29	0.30	1.51	87.28	3.62
3	17.98	0.88	0.42	0.68	0.34	0.11	0.76	4.01	15.74	59.07
4	15.40	1.01	0.36	1.04	0.42	0.36	0.61	3.57	15.87	61.35
5	2.09	2.33	0.20	1.77	1.86	0.28	1.09	9.45	58.19	22.63
6	2.26	2.69	0.60	1.87	1.87	0.52	1.16	10.23	58.78	20.04

The location of the data points is marked in Fig.8b. Indeed, large amounts of W-rich oxide particles exist in the Ni matrix, which separates the Ni matrix into small blocks and prevents the formation of a continuous scale.

Structural stability and oxidation resistance are the key points when we develop the low Cr high W casting superalloys applied at temperatures over 1100°C besides the strength considerations. The excessive alloying by W usually cause the precipitation of α (W, Mo) and μ phases [5] and it can be avoided by modifying the composition of alloys. Although Cr-free IC-6 alloy was applied [6], there is still worry about excessive reduction of the oxidation resistance due to the lower Cr content. Thus, how to affect the oxidation resistance and further improve high temperature strength is the key research topic motivating the substitution of Ru for Ni.

The experimental results indicate that the substitution 3wt%Ru for Ni did not cause the precipitation of any new phases. Ru is a very weak positive segregation element and restricts the formation of M_6C carbide, which is important for solid solution heat treatment and long time service of high W alloys. For high W free-Ru alloys, large blocky M_6C carbides (up to 10μm) were formed after a short time when the temperature is over 1280°C. The content of W in M_6C carbide is up to 70% reducing the W content within matrix and γ' phases. Meanwhile, the presence of both coarsening of M_6C carbides and the formation of M_6C thin films at the grain boundaries and the interdendrite regions also reduce the high temperature stress rupture properties of high W alloys. Thus, it is beneficial for the addition of Ru to restrict and delay the formation of M_6C carbide.

The role of Ru on the improvement of oxidation resistance is not obvious. It slightly delays spalling of the scale, and does not significantly decrease the weight-loss and weight-gain rate. Especially for the alloy containing 1.5Cr, once the protective scale has not formed, the addition of Ru did not improve its oxidation resistance, while the addition of Y can improve the oxidation resistance of Cr-free alloy [7]. It is considered that the contribution to oxidation resistance of Y is superior to that of Ru.

Conclusions

1. Ru is a weak positive segregation element, which hardly enters into carbide, but has higher solubility in γ' and Ni_5Hf phases. The partitioning ratio of Ru in γ/γ' is about 1:0.7.
2. The addition of Ru in low Cr high W alloys can improve the structural stability and delay the M_6C carbide formation. Ru slightly increases the incipient melting temperature of alloys.
3. Ru can delay the oxide scale spalling, but does not reduce the oxidation rate for low Cr high W alloys. With respect to improvement of oxidation resistance, Y is superior to Ru.

Reference

1. W.S. Walston, K.S. O'Hara, E.W. Ross, T.M. Pollock and W.H. Murphy, "RENE N6: Third generation Single Crystal Superalloy", Proc. of the 8th Inter. Symp. on Superalloys, Ed. by R.D. Kissinger et al., TMS, (1996), 27-34.

2. H.E. Collins, "Effect of Thermal Exposure on the Microstructure and Mechanical Properties of Nickel-Base Superalloys", Metall. Trans., 6(1), 1974, 189-204.

3. Zheng Yunrong and Zhang Detang, Colour Metallographic Investigation of Superalloys and Steels (Beijing, National Defence Press, 1999), 2.

4. Xuan Nguyen-Dinh, "Phase Stable Single Crystal Materials", United Stated Patent Number 4, 935, 072, Jun. 19, 1990.

5. Zheng Yunrong, "Primary μ Phase in Cast Nickel Base Superalloys", Acta Metallurgical Sinica, 35(12) (1999), 1242-1245.

6. Y.F. Han, Z.P. Xing and M.C. Chaturvedi, 'Development and Engineering Application of a DS Cast Ni_3Al Alloy IC6", Structural Intermetallics 1997, Ed. by M.V. Nathal et al., TMS(1997), 713-719.

7. C. Xiao and Y.F. Han, "Effect of Yttrium on the Microstructure and Oxidation Resistance of Ni_3Al-Base Alloy IC6", Journal of Materials Engineering, 1998, no.6: 23-28.